OXFORD

Cerebral Cortex, January 2020;30: 382–390

doi: 10.1093/cercor/bhz094
Advance Access Publication Date: 2 July 2019
Original Article

ORIGINAL ARTICLE

Quantitative MRI Analyses of Regional Brain Growth in Living Fetuses with Down Syndrome

Tomo Tarui[1], Kiho Im[2], Neel Madan[3], Rajeevi Madankumar[4], Brian G. Skotko[5], Allie Schwartz[5], Christianne Sharr[5], Steven J. Ralston[6], Rie Kitano[1], Shizuko Akiyama[1], Hyuk Jin Yun[2,], Ellen Grant[2] and Diana W. Bianchi[7]

[1]Mother Infant Research Institute, Fetal Neonatal Neurology Program, Pediatric Neurology, Tufts Medical Center, Boston, MA 02111, USA [2]Fetal-Neonatal Neuroimaging and Developmental Science Center, Division of Newborn Medicine, Boston Children's Hospital, Harvard Medical School, Boston, MA 02115, USA [3]Radiology, Tufts Medical Center, Boston, MA 02111, USA [4]Maternal Fetal Medicine, Obstetrics and Gynecology, Long Island Jewish Medical Center Northwell Health, New Hyde Park, NY 11040, USA [5]Down Syndrome Program, Genetics, Pediatrics, Massachusetts General Hospital, Boston, MA 02114, USA [6]Maternal Fetal Medicine, Obstetrics and Gynecology, University of Pennsylvania, Philadelphia, PA 19104, USA and [7]Prenatal Genomics and Fetal Therapy Section, Medical Genetics Branch, National Human Genome Research Institute, Bethesda, MD 20892, USA

Address correspondence to Tomo Tarui, MD, 800 Washington Street, #394, Boston, MA 02111, USA. E-mail: ttarui@tuftsmedicalcenter.org.

Abstract

Down syndrome (DS) is the most common liveborn autosomal chromosomal anomaly and is a major cause of developmental disability. Atypical brain development and the resulting intellectual disability originate during the fetal period. Perinatal interventions to correct such aberrant development are on the horizon in preclinical studies. However, we lack tools to sensitively measure aberrant structural brain development in living human fetuses with DS. In this study, we aimed to develop safe and precise neuroimaging measures to monitor fetal brain development in DS. We measured growth patterns of regional brain structures in 10 fetal brains with DS (29.1 ± 4.2, weeks of gestation, mean $\pm$ SD, range 21.7∼35.1) and 12 control fetuses (25.2 ± 5.0, range 18.6∼33.3) using regional volumetric analysis of fetal brain MRI. All cases with DS had confirmed karyotypes. We performed non-linear regression models to compare fitted regional growth curves between DS and controls. We found decreased growth trajectories of the cortical plate ($P = 0.033$), the subcortical parenchyma ($P = 0.010$), and the cerebellar hemispheres ($P < 0.0001$) in DS compared to controls. This study provides proof of principle that regional volumetric analysis of fetal brain MRI facilitates successful evaluation of brain development in living fetuses with DS.

Key words: brain development, Down syndrome, fetal MRI, human fetus, volumetric analysis

Introduction

Down syndrome (DS) is the most common liveborn autosomal chromosomal anomaly and a major cause of developmental disability. Annually, about 5000 babies are born with DS in the US (de Graaf et al. 2016; CDC 2018). Recent advances in prenatal screening for DS using sequencing of cell-free DNA in maternal plasma raises the possibility of early interventions to improve neurocognition (Bianchi and Chiu 2018). Individuals with DS are now living longer, with the median life span being 58 years of age (de Graaf et al. 2016). With individuals experiencing a continuum of life-long pathology originating in the fetal period, there is a desire to intervene as early as the fetal period to improve outcomes (Guedj and Bianchi 2013). However, to determine the impact of interventions, it would be helpful to have methods that measure the severity of the phenotype.

Quantitative analyses of brain magnetic resonance imaging (MRI) have been used to document neuropathology in children with DS (Jernigan and Bellugi 1990; Raz et al. 1995; Frangou et al. 1997; Pearlson et al. 1998; Aylward et al. 1999; Pinter et al. 2001; Kates et al. 2002; Rigoldi et al. 2009; Smigielska-Kuzia et al. 2011; Carducci et al. 2013; Lee et al. 2016). Children with DS have smaller frontal and temporal lobes, hippocampus, and cerebellum measured by manual segmentation and volume reconstruction of whole brain and substructures (Jernigan and Bellugi 1990; Raz et al. 1995; Frangou et al. 1997; Pearlson et al. 1998; Aylward et al. 1999; Pinter et al. 2001; Kates et al. 2002; Smigielska-Kuzia et al. 2011) or by whole-brain voxel-based morphometry (Rigoldi et al. 2009; Carducci et al. 2013; Lee et al. 2016).

Brain anatomical changes in people with DS are associated with neurodevelopmental deficits. Decreased cerebellar vermian volume is associated with poorer gait quality (Rigoldi et al. 2009). Decreased regional gray matter T1 signal densities in the frontal and temporal lobes are associated with deficits in linguistic function and short- and long-term memory, respectively (Menghini et al. 2011). Therefore, having a precise anatomical description could eventually allow clinicians to predict the potential degree of developmental disability observed in individuals with DS.

In contrast to information available after birth, little is known about brain development in living fetuses with DS. Most data are derived from fetopsy and not from the observation of living fetuses. Fetopsies have found decreased volumes in the temporal lobes and cerebellum, likely associated with decreased neurogenesis, altered neuronal differentiation, and apoptosis in broad regions of fetal brain (Golden and Hyman 1994; Guihard–Costa et al. 2006; Guidi et al. 2008; Bhattacharyya et al. 2009; Kanaumi et al. 2013; Guidi et al. 2018). These findings suggest that the brain pathology in DS originates in utero and continues over the lifespan. To the best of our knowledge, however, there has been no in vivo MRI study of fetuses with DS. We hypothesize that such a study will enable physicians and scientists to better evaluate and understand human brain development in living fetuses with DS.

Fetal brain MRI is a robust and safe neuroimaging modality to evaluate fetal brain pathologies. One of its advantages over sonography is that post-acquisition quantitative analyses can be performed, such as volumetric and cerebral surface-based analyses (Clouchoux and Limperopoulos 2012; Studholme 2015). Analysis of fetal brain MRIs has successfully detected subtle developmental aberrations in regional structural growth and cerebral sulcal development in fetuses with brain malformations such as cerebral ventriculomegaly (Biegon and Hoffmann 2014; Benkarim et al. 2018), polymicrogyria (Im et al. 2017), and agenesis of corpus callosum (Tarui et al. 2018). One of its advantages over fetopsy is that MRI can be applied safely to living fetuses also allows a study of inter-individual variations at various time points during development.

In this study, we performed post-acquisition semi-manual segmentation and volumetric MRI analyses to precisely measure patterns of regional brain growth in living fetuses with DS from the second to third trimesters of pregnancy.

Materials and Methods

Subjects

The study was approved by the Institutional Review Boards of Tufts Medical Center (TMC) and Boston Children's Hospital (BCH). The inclusion criteria were the following: prenatal diagnosis of DS was made by either positive cell-free DNA screens confirmed by fetal or neonatal karyotype/chromosomal microarrays (CMA) or an initial prenatal diagnostic procedure such as amniocentesis or chorionic villus sampling (CVS), with karyotype-/CMA. Based on professional guidelines and recommendations from the National Society of Genetic Counselors (NSGC) (Wilson et al. 2013), the International Society for Ultrasound in Obstetrics and Gynecology (ISUOG) (Salomon et al. 2014), the Society for Maternal–Fetal Medicine (SMFM) (Society for Maternal–Fetal Medicine Publications Committee. Electronic address eso 2015), and the American College of Medical Genetics and Genomics (ACMG) (Gregg et al. 2016), all women who have positive cell-free DNA screening results for DS were offered amniocentesis or CVS for confirmative diagnosis, although not all of the pregnant women in this study opted to do so. All newborns that did not have confirmative prenatal diagnosis were confirmed with karyotype diagnosis after birth. Prenatal and postnatal diagnosis of major anomalies (congenital heart disorders, gastrointestinal anomalies, etc.) were also recorded (Table 1).

Written informed consent was obtained from the pregnant women whose fetuses were diagnosed with DS at the visit to TMC prior to fetal MRI. One case of fetal MRI with DS was added from the archived radiology images of BCH. Informed consent process was exempt due to retrospective identification of the case. Healthy pregnant women with uncomplicated pregnancies from the obstetric clinic were recruited as controls (CT). Inclusion criteria for pregnant women with DS or CT were: maternal age 18–45 years; gestational age 18–36 weeks. We excluded multiple gestation pregnancies, fetuses with dysmorphic features on ultrasound examination, other brain malformations or brain lesions, and known congenital infections. We also excluded subjects as healthy controls if the fetal MRI identified any abnormality. Images were excluded if significant motion or other artifacts that degraded image quality were present. A pediatric neurologist (T.T.) and a neuroradiologist (N.M.) performed conventional MRI studies to detect associated anomalies.

MRI Acquisition

Fetal brains were scanned using T2 weighted HASTE (half-fourier acquisition single-shot turbo spin-echo) MRI sequence on a Phillips 1.5 T scanner (TMC). One case from BCH was scanned by Siemens Binney 7, Skyra 3 tesla MRI. We used body coils that were routinely used for pelvis MRI. The following

Table 1 Maternal and fetal demographics of fetuses with Down syndrome and typically developing controls

	Subject	Ethnicity	Maternal age	Maternal risks*	CVS/AC/postnatal karyotype	Fetal sex	GA of MRI [weeks]	Other anomalies
Down syndrome	DS-01	White	30	None	47,XX,+21	F	30.86	None
	DS-02	White	33	None	47,XY,+21	M	31.57	None
	DS-03	White	30	None	47,XX,+21	F	29.71	AVCD repaired after birth
	DS-07	White	41	None	47,XX,+21	F	30.00	AVCD repaired after birth
	DS-08	White	33	None	47,XX,+21	F	22.29 & 29.71	ASD, mitral regurgitation, PFO repaired after birth
	DS-10	White	36	None	47,XY,+21	M	21.71	Neonatal pulmonary hypertension
	DS-11	White	34	None	47,XX,+21	F	35.14	None
	DS-13	White	44	None	47,XY,+21	M	27.43	Interrupted aortic arch repaired after birth, hydronephrosis
	BDS-02	White	38	Cymbalta, Lyrica for fibromyalgia	47,XY,+21	M	32.43	Tricuspid regurgitation
Typically Developing Controls	BM-10	White	23	None	N/A	M	20	None
	BM-18	White	30	None	N/A	M	29.57	None
	BM-26	White	31	None	N/A	M	18.57	None
	BM-28	White	32	None	N/A	F	22.86	None
	BM-37	Asian	22	None	N/A	F	29.14	None
	BM-38	Asian	33	None	N/A	F	25.57	None
	BM-39	White	34	None	N/A	M	32	None
	BM-42	White	30	None	N/A	M	33.29	None
	BM-47	White	34	None	N/A	M	24.71	None
	BM-54	White	27	None	N/A	M	19.71	None
	BM-92	African American	22	None	N/A	F	20.86	None
	BM-97	White	31	None	N/A	M	25.71	None

Note: In visual assessment, no cerebral ventriculomegaly nor apparent cerebellar hypoplasia was appreciated. AC: amniocentesis, ASD: atrial septal defect, AVCD: atrioventricular canal defect, CVS: chorionic villi sampling, GA: gestational age, PFO: patent foramen ovale. *Maternal risks: gestational hypertension, diabetes, medications, smoking, alcohol, or recreational drug consumption.

sequence was used for each subject: time repetition = ~12.5 s, time echo = 180 ms, field of view = 256 mm, in-plane resolution = 1 mm, slice thickness = 2–3 mm. The HASTE acquisition was acquired at least 3 times in different orthogonal orientations. In addition to these, 3 to 12 HASTE scans (depending on the severity of the motion artifacts) oriented at ~30°–45° relative to the original 3 orthogonal scans were acquired for reliable image post-processing.

Preprocessing for Quantitative Fetal MRI Analysis

Multiple HASTE acquisitions were processed to correct for slice to slice fetal head motion and to perform isotropic high-resolution volume reconstructions (voxel size: 0.75 × 0.75 × 0.75 [mm]) (Kuklisova-Murgasova et al. 2012; Im et al. 2017; Tarui et al. 2018) (Fig. 1*a*,*b*). Quality of reconstructed volume was visually inspected in focus of continuity of cortical plate, partial volume effect in the boundaries of cortical plate, and cerebrospinal fluid. The volume images of each subject were manually aligned along the anterior and posterior commissure (AC-PC) points using AFNI (afni.nimh.nih.gov/afni) (Cox 2012).

Volumetric Analysis

In coronal images of reconstructed and aligned volume images, the regional structures of the brain—cortical plate, subcortical parenchyma, cerebellar hemispheres, vermis, brainstem, lateral-, third-, and fourth ventricles—were manually segmented on each slice using intensity value ranges and corrected by examining on orthogonal axial and sagittal planes using FreeView (surfer.nmr.mgh.harvard.edu) (Fig.1*d*). Because the signal intensity and anatomical structures recognized in fetal brain is different to adult/matured brain, we did not use signal intensity-based automatic segmentation that is offered by FreeView. All segmentation was done manually. Because of limited tissue contrast, structures such as developing white matter (intermediate zones, subplate, etc.), basal ganglia, etc. were segmented as one subcortical parenchymal region. The border between subcortical parenchyma and brainstem was determined in the coronal plane as the line between the lateral and highest ends of bilateral transverse fissures (Fig.1*c*,*d*). To increase inter-rater reliability, all investigators underwent training segmentations of practice brains to have consistent performance among raters before the actual segmentations of the subjects' data. Regional structural volumes were computed by reconstruction of consecutive planes of segmented coronal images using Slicer 4.8.1 (slicer.org) (Fig. 1*e*).

Surface Area Analysis

Based on segmentation data, the inner cerebral (subcortical parenchyma) surface was extracted using surface-mesh models

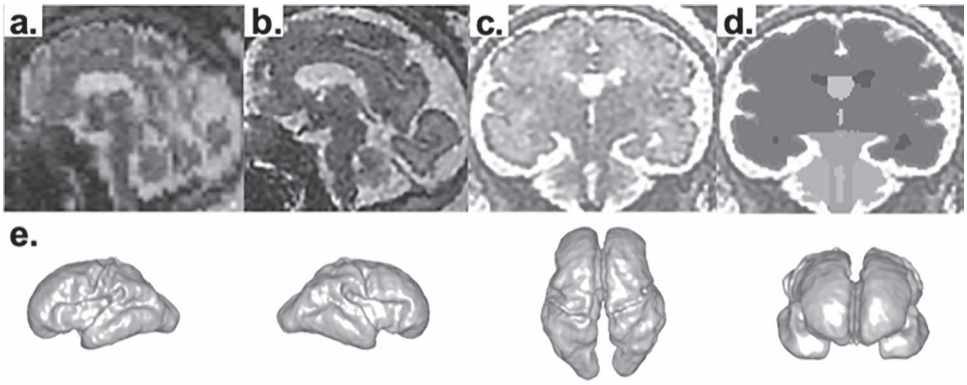

Figure 1. Processing fetal MRI for surface analysis. Raw volume data of fetal MRI (*a*) is processed with motion correction and high-resolution volume reconstruction to reconstruct 3D fetal brain image (*b*). In coronal images of reconstructed volume images (*c*), the regional structures of the brain—cortical plate, subcortical parenchyma, cerebellar hemispheres, vermis, brainstem, lateral-, third-, and fourth ventricles—were manually segmented on each slice using Freeview (*d*). 3D volume rendering of segmentation data of MRI DS08b (*e*).

in each cerebral hemisphere as described previously (Tarui et al. 2018). The inner cerebral surface reflects the gray/white matter border surface. The area of this surface was calculated using Freesurfer (surfer.nmr.mgh.harvard.edu). The thickness of the cortical plate in the second and third trimester (~1 mm) is close to the imaging resolution determined by voxel size (0.75 mm). Therefore, the outer cerebral (pial) surface was not extracted, as it can be distorted by the smoothening process due to the thin cortical plate.

Statistical Analysis

The gestational age distribution between the CT and DS groups was compared using an independent sample *t*-test. Group differences in sex ratios were assessed using a Fisher's exact test. As regional structural volume is significantly associated with gestational age in the fetal period (Clouchoux et al. 2012; Scott et al. 2013), fitted growth curves of regional structures in DS and CT were compared by modeling regional volumes as a function of gestational age using a non-linear regression model. The extra sum-of-squares F test was used to compare a model in which separate best-fit values for some parameters are found for each group, or a model where those parameters are shared among groups. Significance was set at a P-value < 0.05. If the separated curves had a significantly better fit, the CT and DS groups were determined to have distinct growth curves. Inner cerebral surface area was also considered to be a function of gestational age. Best fitted growth curves of inner cerebral surface area in DS and CT were compared using a linear regression model with following equation: Y (surface area) = b0 + b1group + b2age + b3group x age + e. Group differences in slopes and intercepts were tested using Prism (v7.0e, La Jolla, CA) with a P-value < 0.05 set as significance.

For inter-rater reliability test, we calculated Dice's coefficients of regional volume segmentations performed by 2 investigators (between TT and RK, TT and SA) in 4 brains (BM12, BM63, BM92, and DS10).

Results

Subjects

Twenty-five pregnant women were recruited into the study. Of these, 13 were carrying fetuses with DS and 12 were carrying control fetuses. One fetus with DS had two MRIs. Two fetuses with DS died in utero before the fetal MRI scan. One fetus with DS was excluded due to termination of pregnancy before the fetal MRI scan. Two fetal MRIs were severely degraded by artifacts and could not be analyzed. One fetal MRI with DS was added from the archive (confirmed with amniocentesis). As a result, 22 fetal brains were analyzed for volumetrics including 10 fetal brains with DS (13+1-2-1-2+1) and 12 CT fetuses (Supplementary Fig. 1). The demographics of the analyzed cases are summarized in Table 1. The gestational ages of the MRI studies (DS, CT; mean ± SD [range]) were, respectively, 29.1 ± 4.2 (21.7~35.1) and 25.2 ± 5.0 (18.6~33.3) gestational weeks ($P = 0.06$, *t*-test). Fetal sex was not significantly different between fetuses with DS and CT (female DS 50.0%, CT 33.3%, $P = 0.67$, Fisher's exact test). Maternal age was higher in DS compared to CT (35.4 ± 4.8 (30~44), 29.1 ± 4.5 (22~34) year, $P = 0.005$, *t*-test). All pregnancies but one had no associated risk factors such as gestational hypertension, diabetes, medications, smoking, alcohol, or recreational drug consumption. One DS pregnancy (BDS-02) was complicated with maternal fibromyalgia and medications of duloxetine and pregabalin (Table 1). All images were processed for motion correction, volume reconstruction, and AC-PC alignment.

Fetal MRI Findings in DS

There was no ventriculomegaly, defined as atrial width ≧ 10 mm in the coronal plane, detected in fetuses with DS and none developed hydrocephalus by obstetrical ultrasound monitoring. By visual assessment of the MRI, no apparent cerebellar hypoplasia was appreciated, such as cerebellar hemispheric hypoplasia or vermian hypoplasia. The parenchymal signal in the T2 sequence was also normal. Fetal MR images of DS cases are presented in Supplementary Fig. 1.

Volumetric Analysis

Regional volume was considered to be a function of gestational age. Therefore, growth trajectory as a function of gestational age was modeled. Growth trajectories of regional volume were modeled according to non-linear regression models and compared between fetuses with DS and CT. We found exponential curves fit best to gestational age-regional volume

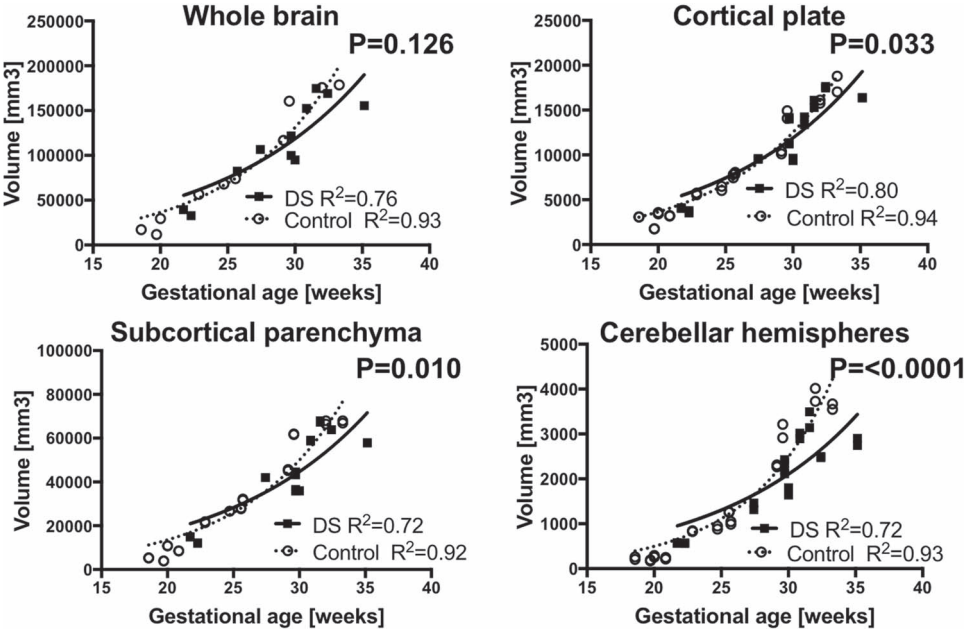

Figure 2. Distinct regional growth trajectories in fetuses with DS and CT. Growth trajectories of regional volume were modeled according to non-linear regression models and compared between fetuses with DS and CT. Growth trajectory of cortical plate (*b*), subcortical parenchyma (*c*), and cerebellar hemispheres (*d*) were significantly smaller in fetuses with DS compared to the CT. Measures from left and right cortical plate, subcortical parenchyma, and cerebellar hemispheres were separately plotted. Growth trajectory of whole brain (*a*) is in different between DS and CT. Volumes of cortical plate, subcortical parenchyma, and cerebellar hemispheres from each hemisphere were plotted separately.

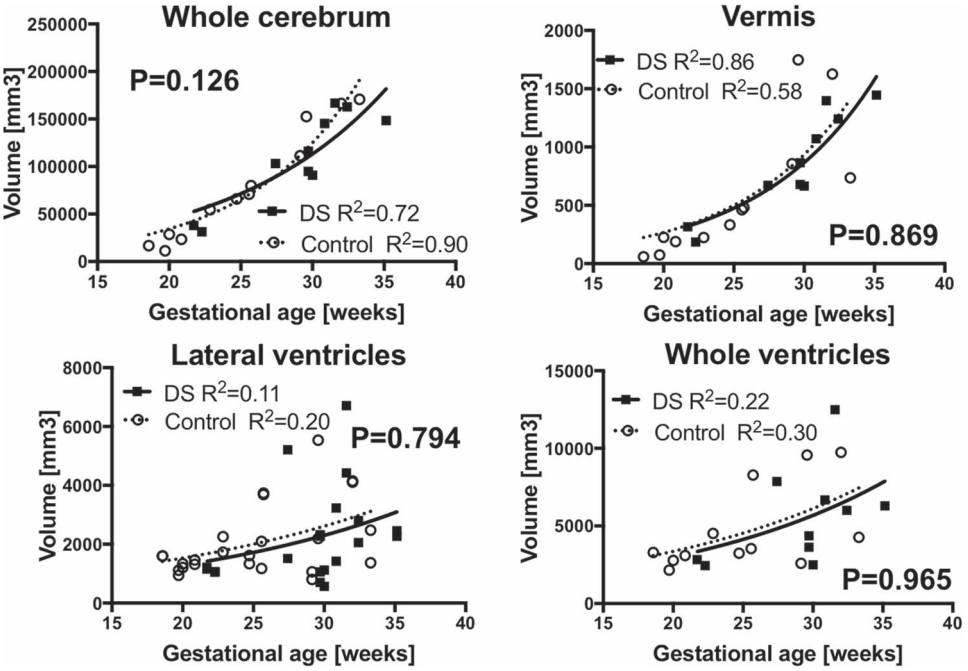

Figure 3. Similar regional growth trajectories in fetuses with DS and CT. Growth trajectory of whole cerebrum (*a*), vermis (*b*), lateral ventricles (*c*), and whole ventricles (*d*) were indifferent between fetuses with DS and the CT. Measures from left and right lateral ventricles were separately plotted.

association in each group: $Y = Y0 * e^{(k*x)}$ (Y: regional volume, X: gestational age, Y0: Y intercept, k: rate constant, CT: R^2 = 0.83∼0.94, DS: 0.69∼0.85). Fetuses with DS had decreased cerebellar hemispheric ($P < 0.0001$), whole cerebellum ($P = 0.043$), cortical plate ($P = 0.033$), and subcortical parenchymal volume ($P = 0.010$) compared to CT. Such differences began around 28 weeks and increased as gestation progressed. No significant differences were observed in whole brain ($P = 0.115$), whole cerebrum ($P = 0.126$), or vermian ($P = 0.869$) volumes (Fig. 2). The growth trajectories of lateral ventricular ($P = 0.794$) or whole ventricular ($P = 0.965$) volumes were not significantly different between DS and CT. However, intragroup variation

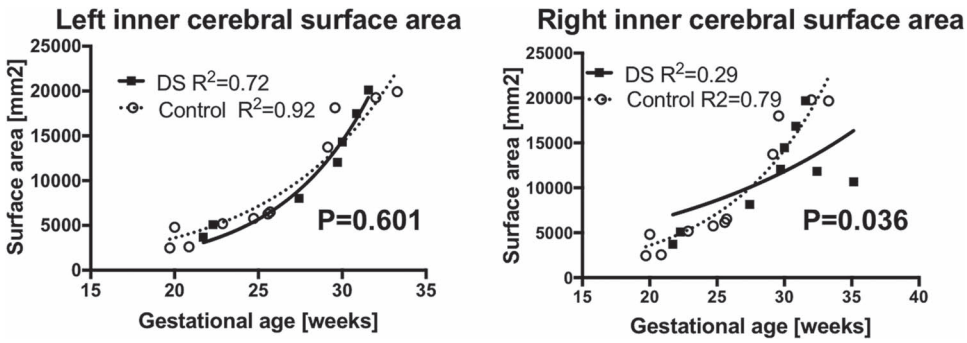

Figure 4. Inner cerebral surface area. Growth trajectory of inner cerebral surface was smaller in right hemispheres (*b*) in fetuses with DS. However, inner surface area of the left hemispheres (*a*) were indifferent between DS and the CT.

was large in both groups, which made group comparison difficult (CT: R^2 = 0.20, 0.30; DS: 0.11, 0.22, respectively) (Fig. 3). We also analyzed growth trajectories of left- and right-sided structures separately for cortical plate, subcortical parenchyma, cerebellar hemispheres, and lateral ventricles. The differences were only significant in right cerebellar hemispheres ($P = 0.015$).

For inter-rater reliability test, Dice's coefficients of regional volume segmentations performed by 2 investigators (between TT and RK, TT and SA) were calculated in 4 brains (BM12, BM63, BM92, and DS10). DICE coefficients ranged as following: left cortical plate 0.942∼0.993, right cortical plate 0.951∼0.988, left subcortical parenchyma 0.988∼0.999, right subcortical parenchyma 0.989∼0.999, left cerebellar hemisphere 0.889∼0.972, and right cerebellar hemisphere 0.883∼0.984.

Surface Area Analysis

The inner cerebral surfaces from 9 of 12 CT and 7 of 10 DS fetal brains were successfully reconstructed. The growth trajectories of inner cerebral surface area were modeled to linear regression models. In the right cerebral hemisphere, fetuses with DS had smaller growth trajectories of the inner cerebral surface area than CT fetuses ($P = 0.036$). In the left cerebral hemisphere, there were no group differences ($P = 0.077$) (Fig. 4).

Discussion

We successfully used quantitative fetal brain MRI analyses of living fetuses with DS to identify decreased cerebral cortical plate, subcortical parenchymal, and cerebellar hemispheric growths compared to CT fetuses. Such changes are detectable after 28 weeks of gestation and increase over time. This study provided proof of principle that fetal brain MRI facilitates successful evaluation of brain development in living fetuses with DS.

Fetal Cerebrum in DS

The findings of the current study are consistent with prior morphological and biometric analyses originating from fetopsy studies in DS. In gross anatomical studies of the cerebrum, biometric measurements of fetopsy specimens identified decreased cerebral and cerebellar sizes during the fetal period, as early as 23 weeks of gestation (Golden and Hyman 1994; Guihard-Costa *et al.* 2006). Histological analyses found reduced cortical plate thickness, less discrete laminar structures, as well as alterations in laminar cell density in the supra temporal gyrus (Golden and Hyman 1994). Such changes appeared to be caused by decreased neurogenesis (Guidi et al. 2008; Guidi et al. 2018) including decreased cortical interneurons (Bhattacharyya et al. 2009) and hippocampal neurons (Guidi et al. 2008). In addition, decreased cells with glial lineages have been documented (Kanaumi et al. 2013). Others have suggested that increased apoptosis can contribute lesser neurons in the developing hippocampi of fetuses with DS (Guidi et al. 2008). Those fetopsy studies detected such developmental alterations as early as 17 weeks (Guidi et al. 2008; Guidi et al. 2011). In this MRI study, decreased regional growths were detected around 28 weeks, which may be either due to the time lag from development of histological changes to macroanatomical changes, or small number of subjects in earlier gestation. Inclusion of larger number of younger gestational age fetuses may possibly detect growth differences in earlier age.

Reduction in cortical volume may be contributed by a reduction in cortical surface area rather than cortical thickness in youth with DS (Lee et al. 2016). We found reduction in the cerebral inner surface area in the right, but not in the left hemisphere. Our method did not allow a measure of cortical plate thickness because the imaging resolution determined by voxel size (0.75 mm) is similar to cortical plate thickness of fetuses in this age range (∼1 mm). We therefore defer the conclusion to a larger scale study to determine if the reduction in cortical volume is due to reduction in surface area or thickness. Further cerebral surface analysis, including sulcal developmental pattern analysis, is under way. We did not find differences in the whole cerebrum volume between fetuses with DS and CT, despite differences in the cortical plate and subcortical parenchyma. This may be due to low power. In the analysis of cortical plate and subcortical parenchyma, we used data from each hemisphere separately, while we measured both hemisphere data to calculate whole cerebrum volume, which resulted in a decrease in data points.

Fetal Subcortical Structures in DS

Growing evidence of fetal white matter developmental anomalies has been reported in animal models of DS (Olmos-Serrano et al. 2016) and human fetopsy studies (Zdaniuk et al. 2011; Kanaumi et al. 2013; Sarnat and Flores-Sarnat 2016). Studies have suggested reduction in non-neuronal cellular proliferation (Kanaumi et al. 2013) and alterations in oligodentrocyte

development (Olmos-Serrano et al. 2016). We found that such cellular level changes in white matter result in a reduction in subcortical parenchymal volume that becomes apparent after 28 weeks. This is consistent with white matter volume reduction observed in volumetric MRI in children with DS (Kates et al. 2002). MRI tissue contrast resolution limits separating developing white matter and other subcortical structures such as basal ganglia. On the other hand, it is a critical advantage of the fetal MRI method that it could non-invasively and sensitively detect another key developmental aberration in DS fetal brains. Implications of each regional growth aberration on specific domains of neurodevelopmental function have yet to be tested in an ongoing longitudinal fetal–neonatal cohort follow-up study.

Fetal Cerebellum in DS

Decreased cerebellar growth is a well-known cardinal feature of fetal brain development in DS. Detailed gross anatomical and histological studies from the Bartesaghi laboratory have identified cerebellar developmental changes such as immature morphology (shallower fissures, reduced number of lobuli) and reduced growth of the cerebellum that is caused by decreased neurogenesis in cerebellar germinal matrix and a resulting reduced neuronal number in the cerebellum (Guidi et al. 2011). However, non-invasive evaluation of fetal cerebellum in DS has been challenging without sufficient sensitivity to detect such differences (Hill et al. 1991). This is a common challenge for obstetric sonography to evaluate posterior fossa structures (Griffiths et al. 2017). In contrast, fetal MRI has an advantage over sonography to evaluate posterior fossa structures, including the cerebellum. Our study has identified lagging cerebellar growth after 28 weeks. In the conventional visual review of fetal MRI, such decreases in cerebellar volume are not appreciated. Although decreased growth in the cortical plate, subcortical parenchyma, and cerebellum were recognized in our quantitative fetal brain MRI analyses, these observations were based on small number of cases. A larger scale study is needed to determine the range of variable growth patterns in each individual fetus and their association with future neurodevelopmental outcomes.

Life-Long Continuum of Brain Pathology in DS

Our observation of decreased cerebral cortical plate, subcortical parenchymal, and cerebellar development is consistent with observations in older children. Children with DS (mean age 11.3 ± 5.2 years, 6.7 ± 3.7 years, in subsequent studies) have reduced volumes in the hippocampus and frontal and temporal lobes (Pinter et al. 2001; Smigielska-Kuzia et al. 2011). At older ages, such changes were also seen in adult individuals with DS without dementia (age range 25.3–62.5 years), as reductions of cerebellum, cingulate gyrus, left medial frontal lobe, right middle/superior temporal gyrus, and left CA2/CA3 regions of hippocampus (White et al. 2003; Teipel et al. 2004).

We believe that decreased subcortical parenchymal growth is a novel finding in fetuses with DS. In older children, white matter volumes were also reduced in cerebellum, frontal and parietal lobes, sub-lobar regions, and brainstem (Carducci et al. 2013). Therefore, white matter changes observed in the fetal period may also result in life-long pathology in DS from the fetal to postnatal periods. Putting all of these findings and our data together, we hypothesize that the neuropathology of DS is a life-long continuum that originates in the fetal period as early as 28 weeks and continues toward childhood and adulthood. It has phases of developmental, maturational, and degenerative processes that overlap and transition one to another. It is important to understand this continuum for development of therapies for DS targeting neuropathology and to designing drug that are specific for each developmental stage.

At this moment, the quantitative fetal MRI method has limitations in resolution. Our method is unable to segment smaller substructures, such as basal ganglia and the hippocampus, which may be a region of interest to sensitively detect pathological changes of DS. We are developing regional analytic methods to implement both volumetric and sulcal development analyses.

In this study, we identified developmental differences between fetuses with and without DS. To utilize such precise anatomical information in association with an individual's neurodevelopmental outcomes, future studies will need to detect inter-individual variations in brain development as well as to follow cohorts through childhood to associate their developmental outcomes.

Supplementary Material

Supplementary material is available at *Cerebral Cortex* online.

Funding

This work was supported by National Institutes of Health K23HD079605, R21HD083956, Jerome Lejeune Foundation, and the Susan Saltonstall Foundation.

Notes

The authors thank Michael Stanley, Annie Felhofer, Jiyeon Janice Jang, and Esther Muradov, for their help with the post-acquisition segmentation of fetal brain MRI, Drs Ada Taymoori and Vidya Iyer for helping identification and recruitment of the participants.

References

Aylward EH, Li Q, Honeycutt NA, Warren AC, Pulsifer MB, Barta PE, Chan MD, Smith PD, Jerram M, Pearlson GD. 1999. MRI volumes of the hippocampus and amygdala in adults with Down's syndrome with and without dementia. *Am J Psychiatry*. 156:564–568.

Benkarim OM, Hahner N, Piella G, Gratacos E, Gonzalez Ballester MA, Eixarch E, Sanroma G. 2018. Cortical folding alterations in fetuses with isolated non-severe ventriculomegaly. *Neuroimage Clin*. 18:103–114.

Bhattacharyya A, McMillan E, Chen SI, Wallace K, Svendsen CN. 2009. A critical period in cortical interneuron neurogenesis in down syndrome revealed by human neural progenitor cells. *Dev Neurosci*. 31:497–510.

Bianchi DW, Chiu RWK. 2018. Sequencing of circulating cell-free DNA during pregnancy. *N Engl J Med*. 379:464–473.

Biegon A, Hoffmann C. 2014. Quantitative magnetic resonance imaging of the fetal brain in utero: methods and applications. *World J Radiol*. 6:523–529.

Carducci F, Onorati P, Condoluci C, Di Gennaro G, Quarato PP, Pierallini A, Sara M, Miano S, Cornia R, Albertini G. 2013.

Whole-brain voxel-based morphometry study of children and adolescents with Down syndrome. *Funct Neurol*. 28:19–28.

Centers for Disease Control and Prevention. 2018. *Facts about Down Syndrome*. In. Birth Defects Homepage. https://www.cdc.gov/ncbddd/birthdefects/downsyndrome.html.

Clouchoux C, Kudelski D, Gholipour A, Warfield SK, Viseur S, Bouyssi-Kobar M, Mari JL, Evans AC, du Plessis AJ, Limperopoulos C. 2012. Quantitative in vivo MRI measurement of cortical development in the fetus. *Brain Struct Funct*. 217: 127–139.

Clouchoux C, Limperopoulos C. 2012. Novel applications of quantitative MRI for the fetal brain. *Pediatr Radiol*. 42(Suppl 1): S24–S32.

Cox RW. 2012. AFNI: what a long strange trip it's been. *Neuroimage*. 62:743–747.

de Graaf G, Buckley F, Skotko BG. 2016. Live births, natural losses, and elective terminations with Down syndrome in Massachusetts. *Genet Med*. 18:459–466.

Frangou S, Aylward E, Warren A, Sharma T, Barta P, Pearlson G. 1997. Small planum temporale volume in Down's syndrome: a volumetric MRI study. *Am J Psychiatry*. 154:1424–1429.

Golden JA, Hyman BT. 1994. Development of the superior temporal neocortex is anomalous in trisomy 21. *J Neuropathol Exp Neurol*. 53:513–520.

Gregg AR, Skotko BG, Benkendorf JL, Monaghan KG, Bajaj K, Best RG, Klugman S, Watson MS. 2016. Noninvasive prenatal screening for fetal aneuploidy, 2016 update: a position statement of the American College of Medical Genetics and Genomics. *Genet Med*. 18:1056–1065.

Griffiths PD, Brackley K, Bradburn M, Connolly DJA, Gawne-Cain ML, Kilby MD, Mandefield L, Mooney C, Robson SC, Vollmer B, *et al*. 2017. Anatomical subgroup analysis of the MERIDIAN cohort: posterior fossa abnormalities. *Ultrasound Obstet Gynecol*.E 50:745–752.

Guedj F, Bianchi DW. 2013. Noninvasive prenatal testing creates an opportunity for antenatal treatment of Down syndrome. *Prenat Diagn*. 33:614–618.

Guidi S, Bonasoni P, Ceccarelli C, Santini D, Gualtieri F, Ciani E, Bartesaghi R. 2008. Neurogenesis impairment and increased cell death reduce total neuron number in the hippocampal region of fetuses with Down syndrome. *Brain Pathol*. 18:180–197.

Guidi S, Ciani E, Bonasoni P, Santini D, Bartesaghi R. 2011. Widespread proliferation impairment and hypocellularity in the cerebellum of fetuses with Down syndrome. *Brain Pathol*. 21:361–373.

Guidi S, Giacomini A, Stagni F, Emili M, Uguagliati B, Bonasoni MP, Bartesaghi R. 2018. Abnormal development of the inferior temporal region in fetuses with Down syndrome. *Brain Pathol*. 140:378–391.

Guihard-Costa AM, Khung S, Delbecque K, Menez F, Delezoide AL. 2006. Biometry of face and brain in fetuses with trisomy 21. *Pediatr Res*. 59:33–38.

Hill LM, Rivello D, Peterson C, Marchese S. 1991. The transverse cerebellar diameter in the second trimester is unaffected by Down syndrome. *Am J Obstet Gynecol*. 164:101–103.

Im K, Guimaraes A, Kim Y, Cottrill E, Gagoski B, Rollins C, Ortinau C, Yang E, Grant PE. 2017. Quantitative folding pattern analysis of early primary sulci in human fetuses with brain abnormalities. *AJNR Am J Neuroradiol*. 38:1449–1455.

Jernigan TL, Bellugi U. 1990. Anomalous brain morphology on magnetic resonance images in Williams syndrome and Down syndrome. *Arch Neurol*. 47:529–533.

Kanaumi T, Milenkovic I, Adle-Biassette H, Aronica E, Kovacs GG. 2013. Non-neuronal cell responses differ between normal and Down syndrome developing brains. *Int J Dev Neurosci*. 31: 796–803.

Kates WR, Folley BS, Lanham DC, Capone GT, Kaufmann WE. 2002. Cerebral growth in Fragile X syndrome: review and comparison with Down syndrome. *Microsc Res Tech*. 57:159–167.

Kuklisova-Murgasova M, Quaghebeur G, Rutherford MA, Hajnal JV, Schnabel JA. 2012. Reconstruction of fetal brain MRI with intensity matching and complete outlier removal. *Med Image Anal*. 16:1550–1564.

Lee NR, Adeyemi EI, Lin A, Clasen LS, Lalonde FM, Condon E, Driver DI, Shaw P, Gogtay N, Raznahan A *et al*. 2016. Dissociations in cortical morphometry in youth with Down syndrome: evidence for reduced surface area but increased thickness. *Cereb Cortex*. 26:2982–2990.

Menghini D, Costanzo F, Vicari S. 2011. Relationship between brain and cognitive processes in Down syndrome. *Behav Genet*. 41:381–393.

Olmos-Serrano JL, Kang HJ, Tyler WA, Silbereis JC, Cheng F, Zhu Y, Pletikos M, Jankovic-Rapan L, Cramer NP, Galdzicki Z *et al*. 2016. Down syndrome developmental brain transcriptome reveals defective oligodendrocyte differentiation and myelination. *Neuron*. 89:1208–1222.

Pearlson GD, Breiter SN, Aylward EH, Warren AC, Grygorcewicz M, Frangou S, Barta PE, Pulsifer MB. 1998. MRI brain changes in subjects with Down syndrome with and without dementia. *Dev Med Child Neurol*. 40:326–334.

Pinter JD, Brown WE, Eliez S, Schmitt JE, Capone GT, Reiss AL. 2001. Amygdala and hippocampal volumes in children with Down syndrome: a high-resolution MRI study. *Neurology*. 56:972–974.

Raz N, Torres IJ, Briggs SD, Spencer WD, Thornton AE, Loken WJ, Gunning FM, McQuain JD, Driesen NR, Acker JD. 1995. Selective neuroanatomic abnormalities in Down's syndrome and their cognitive correlates: evidence from MRI morphometry. *Neurology*. 45:356–366.

Rigoldi C, Galli M, Condoluci C, Carducci F, Onorati P, Albertini G. 2009. Gait analysis and cerebral volumes in Down's syndrome. *Funct Neurol*. 24:147–152.

Salomon LJ, Alfirevic Z, Audibert F, Kagan KO, Paladini D, Yeo G, Raine-Fenning N, Committee ICS. 2014. ISUOG consensus statement on the impact of non-invasive prenatal testing (NIPT) on prenatal ultrasound practice. *Ultrasound Obstet Gynecol*. 44:122–123.

Sarnat HB, Flores-Sarnat L. 2016. Synaptogenesis and myelination in the nucleus/tractus solitarius: potential role in apnea of prematurity, congenital central hypoventilation, and sudden infant death syndrome. *J Child Neurol*. 31:722–732.

Scott JA, Habas PA, Rajagopalan V, Kim K, Barkovich AJ, Glenn OA, Studholme C. 2013. Volumetric and surface-based 3D MRI analyses of fetal isolated mild ventriculomegaly: brain morphometry in ventriculomegaly. *Brain Struct Funct*. 218:645–655.

Smigielska-Kuzia J, Bockowski L, Sobaniec W, Sendrowski K, Olchowik B, Cholewa M, Lukasiewicz A, Lebkowska U. 2011. A volumetric magnetic resonance imaging study of brain structures in children with Down syndrome. *Neurol Neurochir Pol*. 45:363–369.

Society for Maternal-Fetal Medicine Publications Committee. Electronic address eso. 2015. SMFM Statement: clarification of recommendations regarding cell-free DNA aneuploidy screening. *Am J Obstet Gynecol*. 213:753–754.

Studholme C. 2015. Mapping the developing human brain in utero using quantitative MR imaging techniques. *Semin Perinatol*. 39:105–112.

Tarui T, Madan N, Farhat N, Kitano R, Ceren Tanritanir A, Graham G, Gagoski B, Craig A, Rollins CK, Ortinau C *et al.* 2018. Disorganized patterns of sulcal position in fetal brains with agenesis of corpus callosum. *Cereb Cortex*. 28:3192–3203.

Teipel SJ, Alexander GE, Schapiro MB, Moller HJ, Rapoport SI, Hampel H. 2004. Age-related cortical grey matter reductions in non-demented Down's syndrome adults determined by MRI with voxel-based morphometry. *Brain*. 127:811–824.

White NS, Alkire MT, Haier RJ. 2003. A voxel-based morphometric study of nondemented adults with Down syndrome. *Neuroimage*. 20:393–403.

Wilson KL, Czerwinski JL, Hoskovec JM, Noblin SJ, Sullivan CM, Harbison A, Campion MW, Devary K, Devers P, Singletary CN. 2013. NSGC practice guideline: prenatal screening and diagnostic testing options for chromosome aneuploidy. *J Genet Couns*. 22:4–15.

Zdaniuk G, Wierzba-Bobrowicz T, Szpak GM, Stepien T. 2011. Astroglia disturbances during development of the central nervous system in fetuses with Down's syndrome. *Folia Neuropathol*. 49:109–114.